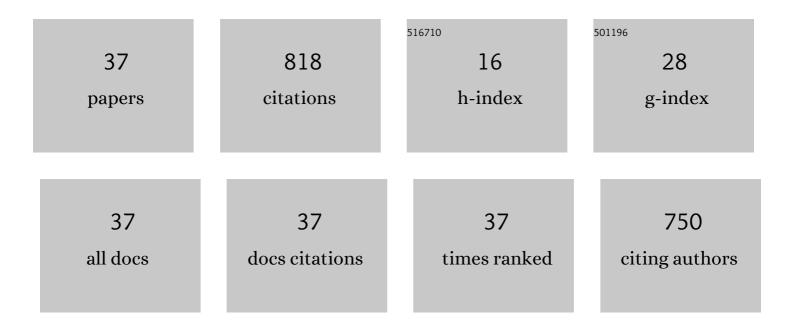


List of Publications by Year in descending order

Source: https://exaly.com/author-pdf/4743872/publications.pdf Version: 2024-02-01



XIANC YI

#	Article	IF	CITATIONS
1	A 57.9-to-68.3 GHz 24.6 mW Frequency Synthesizer With In-Phase Injection-Coupled QVCO in 65 nm CMOS Technology. IEEE Journal of Solid-State Circuits, 2014, 49, 347-359.	5.4	137
2	Pole-Converging Intrastage Bandwidth Extension Technique for Wideband Amplifiers. IEEE Journal of Solid-State Circuits, 2017, 52, 769-780.	5.4	75
3	An 88.5–110 GHz CMOS Low-Noise Amplifier for Millimeter-Wave Imaging Applications. IEEE Microwave and Wireless Components Letters, 2016, 26, 134-136.	3.2	65
4	A 220-to-320-GHz FMCW Radar in 65-nm CMOS Using a Frequency-Comb Architecture. IEEE Journal of Solid-State Circuits, 2021, 56, 327-339.	5.4	52
5	Filling the Gap: Silicon Terahertz Integrated Circuits Offer Our Best Bet. IEEE Microwave Magazine, 2019, 20, 80-93.	0.8	44
6	A 52–57 GHz 6-Bit Phase Shifter With Hybrid of Passive and Active Structures. IEEE Microwave and Wireless Components Letters, 2018, 28, 236-238.	3.2	37
7	A Low-Power Low-Phase-Noise VCO With Self-Adjusted Active Resistor. IEEE Microwave and Wireless Components Letters, 2016, 26, 201-203.	3.2	34
8	Design of Ultra-Low Phase Noise and High Power Integrated Oscillator in \$0.25~mu{m m}\$ GaN-on-SiC HEMT Technology. IEEE Microwave and Wireless Components Letters, 2014, 24, 120-122.	3.2	32
9	Emerging Terahertz Integrated Systems in Silicon. IEEE Transactions on Circuits and Systems I: Regular Papers, 2021, 68, 3537-3550.	5.4	31
10	An on-chip fully electronic molecular clock based on sub-terahertz rotational spectroscopy. Nature Electronics, 2018, 1, 421-427.	26.0	29
11	A Compact 57–67 GHz Bidirectional LNAPA in 65-nm CMOS Technology. IEEE Microwave and Wireless Components Letters, 2016, 26, 628-630.	3.2	25
12	Design of Ring-Oscillator-Based Injection-Locked Frequency Dividers With Single-Phase Inputs. IEEE Microwave and Wireless Components Letters, 2011, 21, 559-561.	3.2	23
13	A High-Efficiency 142–182-GHz SiGe BiCMOS Power Amplifier With Broadband Slotline-Based Power Combining Technique. IEEE Journal of Solid-State Circuits, 2022, 57, 371-384.	5.4	21
14	A 93.4–104.8-GHz 57-mW Fractional-\${N}\$ Cascaded PLL With True In-Phase Injection-Coupled QVCO in 65-nm CMOS Technology. IEEE Transactions on Microwave Theory and Techniques, 2019, 67, 2370-2381.	4.6	20
15	A 24/77 GHz Dual-Band Receiver for Automotive Radar Applications. IEEE Access, 2019, 7, 48053-48059.	4.2	18
16	Chip-Scale Molecular Clock. IEEE Journal of Solid-State Circuits, 2019, 54, 914-926.	5.4	18
17	A Carrier Aggregation Transmitter Front End for 5-GHz WLAN 802.11ax Application in 40-nm CMOS. IEEE Transactions on Microwave Theory and Techniques, 2020, 68, 264-276.	4.6	14
18	A 0.31-THz Orbital-Angular-Momentum (OAM) Wave Transceiver in CMOS With Bits-to-OAM Mode Mapping. IEEE Journal of Solid-State Circuits, 2022, 57, 1344-1357.	5.4	13

XIANG YI

#	Article	IF	CITATIONS
19	Design of an oscillator with low phase noise and medium output power in a 0.25 µm GaNâ€onâ€SiC high electronâ€mobility transistors technology. IET Microwaves, Antennas and Propagation, 2015, 9, 795-801.	1.4	12
20	A 100-GHz 0.21-K NETD 0.9-mW/pixel Charge-Accumulation Super-Regenerative Receiver in 65-nm CMOS. IEEE Microwave and Wireless Components Letters, 2016, 26, 531-533.	3.2	11
21	Heterogeneous Integration of GaN and BCD Technologies and Its Applications to High Conversion-Ratio DC–DC Boost Converter IC. IEEE Transactions on Power Electronics, 2019, 34, 1993-1996.	7.9	11
22	A 34-dB Dynamic Range 0.7-mW Compact Switched-Capacitor Power Detector in 65-nm CMOS. IEEE Transactions on Power Electronics, 2019, 34, 9365-9368.	7.9	11
23	A Compact Single Stage V-Band CMOS Injection-Locked Power Amplifier With 17.3% Efficiency. IEEE Microwave and Wireless Components Letters, 2014, 24, 182-184.	3.2	10
24	Reconfigurable 2.4-/5-GHz Dual-Band Transmitter Front-End Supporting 1024-QAM for WLAN 802.11ax Application in 40-nm CMOS. IEEE Transactions on Microwave Theory and Techniques, 2020, 68, 4018-4030.	4.6	10
25	A W-Band Switch-Less Dicke Receiver for Millimeter-Wave Imaging in 65 nm CMOS. IEEE Access, 2018, 6, 39233-39240.	4.2	9
26	An Inverted Ring Oscillator Noise-Shaping Time-to-Digital Converter With In-Band Noise Reduction and Coherent Noise Cancellation. IEEE Transactions on Circuits and Systems I: Regular Papers, 2020, 67, 686-698.	5.4	9
27	A 100 GHz transformer-based varactor-less VCO with 11.2% tuning range in 65nm CMOS technology. , 2012, , .		8
28	A Terahertz Molecular Clock on CMOS Using High-Harmonic-Order Interrogation of Rotational Transition for Medium-/Long-Term Stability Enhancement. IEEE Journal of Solid-State Circuits, 2021, 56, 566-580.	5.4	8
29	A 2.6–3.4 GHz Fractional- \$N\$ Sub-Sampling Phase-Locked Loop Using a Calibration-Free Phase-Switching-Sub-Sampling Technique. IEEE Microwave and Wireless Components Letters, 2018, 28, 147-149.	3.2	5
30	Compact Switched-Capacitor Power Detector With Frequency Compensation in 65-nm CMOS. IEEE Access, 2020, 8, 34197-34203.	4.2	4
31	A Parallel Sliding-IF Receiver Front-End With Sub-2-dB Noise Figure for 5–6-GHz WLAN Carrier Aggregation. IEEE Journal of Solid-State Circuits, 2021, 56, 392-403.	5.4	4
32	Realization of In-Band Full-Duplex Operation at 300 and 4.2 K Using Bilateral Single-Sideband Frequency Conversion. IEEE Journal of Solid-State Circuits, 2021, 56, 1387-1397.	5.4	4
33	A Current-Reused VCO With Inductive-Transformer Feedback Technique. IEEE Transactions on Microwave Theory and Techniques, 2022, 70, 2680-2689.	4.6	4
34	A divide-by-two injection-locked frequency divider with 13-GHz locking range in 0.18-μm CMOS technology. , 2011, , .		3
35	An Eight-Phase In-Phase Injection-Coupled VCO in 65-nm CMOS Technology. IEEE Microwave and Wireless Components Letters, 2017, 27, 299-301.	3.2	3
36	A 3.4–4.6GHz In-Band Full-Duplex Front-End in CMOS Using a Bi-Directional Frequency Converter. , 2020		2

#	Article	IF	CITATIONS
37	A VCO With Extra Cross-Coupling Path. IEEE Microwave and Wireless Components Letters, 2021, 31, 1130-1133.	3.2	2